



**alpha,omega-Bis(trialkoxysilyl) difunctionalized
polycyclooctenes from ruthenium-catalyzed
chain-transfer ring-opening metathesis polymerization**

Xiaolu Michel, Stéphane Fouquay, Guillaume Michaud, Frédéric Simon,
Jean-Michel Brusson, Jean-François Carpentier, Sophie M. Guillaume

► **To cite this version:**

Xiaolu Michel, Stéphane Fouquay, Guillaume Michaud, Frédéric Simon, Jean-Michel Brusson, et al..
alpha,omega-Bis(trialkoxysilyl) difunctionalized polycyclooctenes from ruthenium-catalyzed chain-
transfer ring-opening metathesis polymerization. *Polymer Chemistry*, 2016, 7 (29), pp.4810–4823.
10.1039/c6py00849f . hal-01357417

HAL Id: hal-01357417

<https://hal-univ-rennes1.archives-ouvertes.fr/hal-01357417>

Submitted on 2 Dec 2016

HAL is a multi-disciplinary open access archive for the deposit and dissemination of scientific research documents, whether they are published or not. The documents may come from teaching and research institutions in France or abroad, or from public or private research centers.

L'archive ouverte pluridisciplinaire **HAL**, est destinée au dépôt et à la diffusion de documents scientifiques de niveau recherche, publiés ou non, émanant des établissements d'enseignement et de recherche français ou étrangers, des laboratoires publics ou privés.

α,ω -Bis(Trialkoxysilyl) Difunctionalized Polycyclooctenes from Ruthenium-Catalyzed Chain-Transfer Ring-Opening Metathesis Polymerization

Xiaolu Michel,^a Stéphane Fouquay,^b Guillaume Michaud,^c Frédéric Simon,^c Jean-Michel Brusson,^d
Jean-François Carpentier,^{a,*} and Sophie M. Guillaume^{a,*}

^a Institut des Sciences Chimiques de Rennes (ISCR), UMR 6226 CNRS - Université de Rennes 1,
Campus de Beaulieu, 263 Avenue du Général Leclerc, F-35042 Rennes Cedex, France

^b BOSTIK S.A., 253, Avenue du Président Wilson, F-93211 La Plaine Saint-Denis, France

^c BOSTIK, ZAC du Bois de Plaisance, 101, Rue du Champ Cailloux, F-60280 Venette, France

^d Total S.A., Corporate Science, Tour Michelet A, 24 Cours Michelet – La Défense 10, F-92069
Paris La Défense Cedex, France

* Corresponding authors: jean-francois.carpentier@univ-rennes1.fr; sophie.guillaume@univ-rennes1.fr

Abstract.

The ring-opening metathesis polymerization/cross-metathesis (ROMP/CM) of cyclooctene (COE) using bis(trialkoxysilyl)alkenes as chain-transfer agents (CTAs) and Ru catalysts to afford difunctionalized polyolefins is reported. Formation of telechelic α,ω -bis(trialkoxysilyl) polycycloolefins (**DF**) with controlled molar mass values takes place quite selectively (> 90wt%), along with minor amounts of cyclic non-functionalized polymers (**CNF**), as evidenced by NMR, MALDI-ToF MS, SEC analyses and fractionation experiments. The nature of the CTA and catalyst influenced much the efficiency and selectivity of the reaction. $(\text{MeO})_3\text{SiCH}_2\text{CH}=\text{CHCH}_2\text{Si}(\text{OMe})_3$ (**2**) and $(\text{MeO})_3\text{Si}(\text{CH}_2)_3\text{NHC}(\text{O})\text{OCH}_2\text{CH}=\text{CHCH}_2\text{OC}(\text{O})\text{NH}(\text{CH}_2)_3\text{Si}(\text{OMe})_3$ (**5**) proved the most efficient CTAs in terms of reactivity, catalyst productivity and selectivity towards **DF**. Diurethane CTA **5** is easily prepared, and can also be conveniently generated *in situ* during the ROMP/CM. Grubbs' 2nd-generation catalyst (**G2**) and Hoveyda-Grubbs's catalyst (**HG2**) afforded the best compromise in terms of selectivity and productivity, with turnover numbers up to 95 000 mol(COE).mol(Ru)⁻¹ and 5 000 mol(CTA).mol(Ru)⁻¹.

Keywords: alkoxysilyl, chain-transfer agent, polycyclooctene, ring-opening metathesis polymerization (ROMP), ruthenium catalyst, telechelic polymer

Introduction

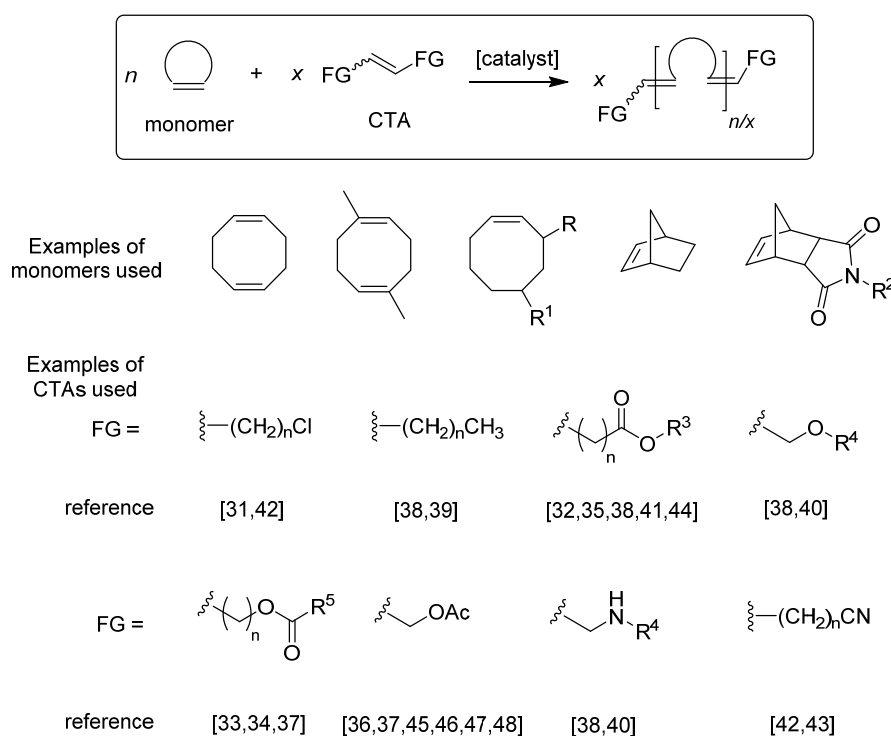
Alkoxysilyl-functionalized polymers are widely used in sealing and adhesive applications. Upon polycondensation of alkoxysilyl groups under the action of moisture, the resulting siloxane network structure ensures a successful and resistant assembly.^{1,2} Several methods are known to prepare alkoxysilyl-functionalized polyolefins. One relies on living anionic polymerization of alkoxysilyl-vinyl or -diene monomers, to generate polymers with alkoxysilyl pendant functions.^{3,4,5,6,7,8,9,10} Post-polymerization reactions of alkali metal-terminated polymers using chlorotrialkoxysilane or tetraalkoxysilane offer an efficient approach toward alkoxysilyl end-functionalized polymers.^{11, 12, 13, 14} Alkoxysilyl-functionalized polymers can also be generated by free-radical polymerization of alkoxysilyl-diene monomers.^{11,13, 15, 16, 17, 18} Hydrosilylation provides another efficient entry towards alkoxysilyl functionalized polymers; for instance, the highly selective hydrosilylation of 1,2-polybutadiene with hydroalkoxysilanes has been described using recyclable Pt nanoclusters as catalysts.¹⁹ Finally, ruthenium-catalyzed cationic polymerization of vinyl ethers using various hydrosilanes as initiator has been reported.²⁰

Acyclic diene metathesis (ADMET) polymerization, as pioneered by Wagener *et al.*, is also an effective route towards polyolefins incorporating alkoxysilyl groups on the terminus(i) or/and in their backbone.²¹ Hence, multi-substituted unsaturated polycarbosilanes have been prepared by one-pot nucleophilic substitution/ADMET polycondensation.^{22,23,24} Similarly, latent reactive processable elastomers constructed of carbosilane or carbosiloxane and polyether segments have been synthesized by using “chain-internal” and “chain-end” reactive methoxysilyl functionalities.^{25,26,27} Also, α,ω -bis(trialkylsilyl) telechelic polybutadienes with tailored molar mass have been synthesized via ADMET depolymerization of 1,4-polybutadiene in the presence of 1,5-di(*tert*-butyldimethylsilyl)-3-hexene.^{28,29}

Tandem ring-opening metathesis polymerization (ROMP)/cross-metathesis (CM) of cycloolefins in presence of functional olefins as chain-transfer agents (CTAs) is another

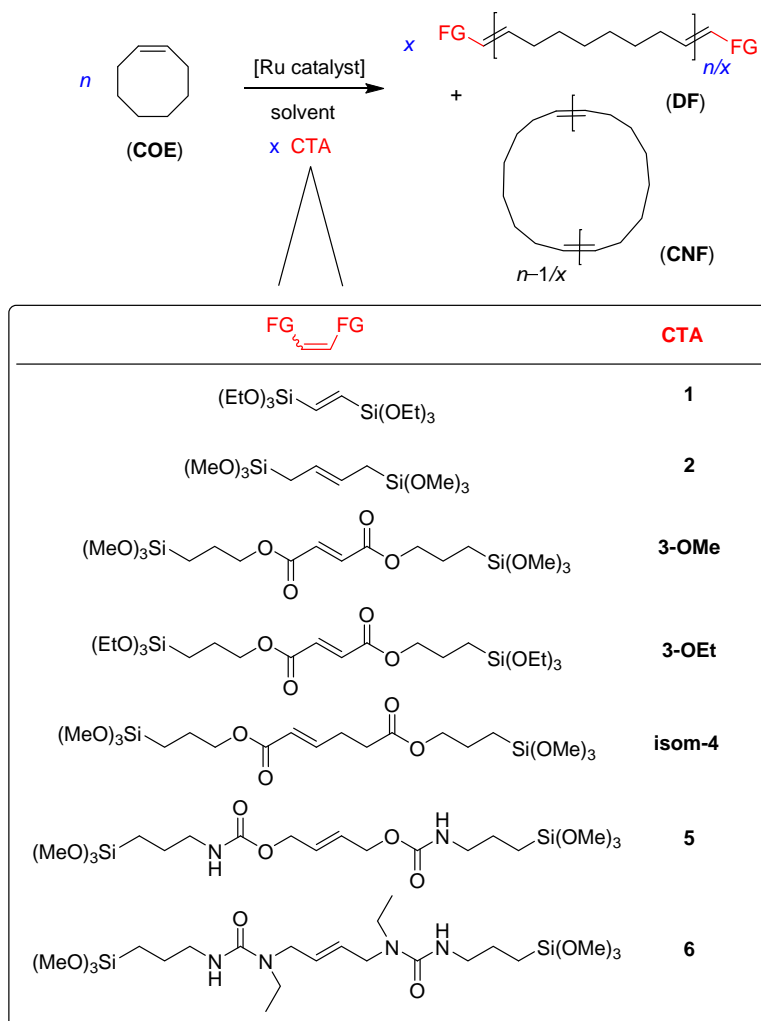
methodology that provides large avenues for the synthesis of silyl-functionalized polyolefins. We have thus reported recently that the Ru-catalyzed ROMP/CM of cyclooctene (COE) using trialkoxysilyl-vinyl type compounds as CTAs effectively leads to the corresponding trialkoxysilyl-functionalized polyolefins;³⁰ the process is, however, unselective as mixtures of α -mono- and α,ω -difunctionalized linear polyolefins, along with lower amounts of isomerized and non-functionalized (linear and cyclic) polymers are formed.

On the other hand, the use of *symmetrically* disubstituted acyclic olefins as CTAs in ROMP/CM process has been reported to form quite selectively α,ω -difunctionalized telechelic polymers (Scheme 1).^{31, 32, 33, 34, 35, 36, 37, 38, 39, 40, 41, 42, 43, 44} For instance, dihydroxy telechelic polyenes have been obtained *via* the Ru-catalyzed ROMP/CM of COE,⁴⁵ 1,5-cyclooctadiene^{46, 47} or 1,5-dimethyl-1,5-cyclooctadiene⁴⁸ using *cis*-1,4-bis(acetoxy)-2-butene as CTA, followed by deprotection of the acetoxy groups.



Scheme 1. Examples of preparation of α,ω -difunctionalized polyenes *via* ROMP/CM of a cycloolefin using a symmetrically disubstituted olefin as chain-transfer agent (CTA).³¹⁻⁴⁸

We now report on the first selective synthesis of α,ω -bis(trialkoxysilyl) telechelic polyolefins using several bis(trialkoxysilyl) olefins as CTAs in the Ru-catalyzed ROMP/CM of COE (Scheme 2). Different types of CTAs and catalysts have been investigated so as to optimize the overall catalytic productivity, selectivity and degree of control over the resulting telechelic macromolecules.

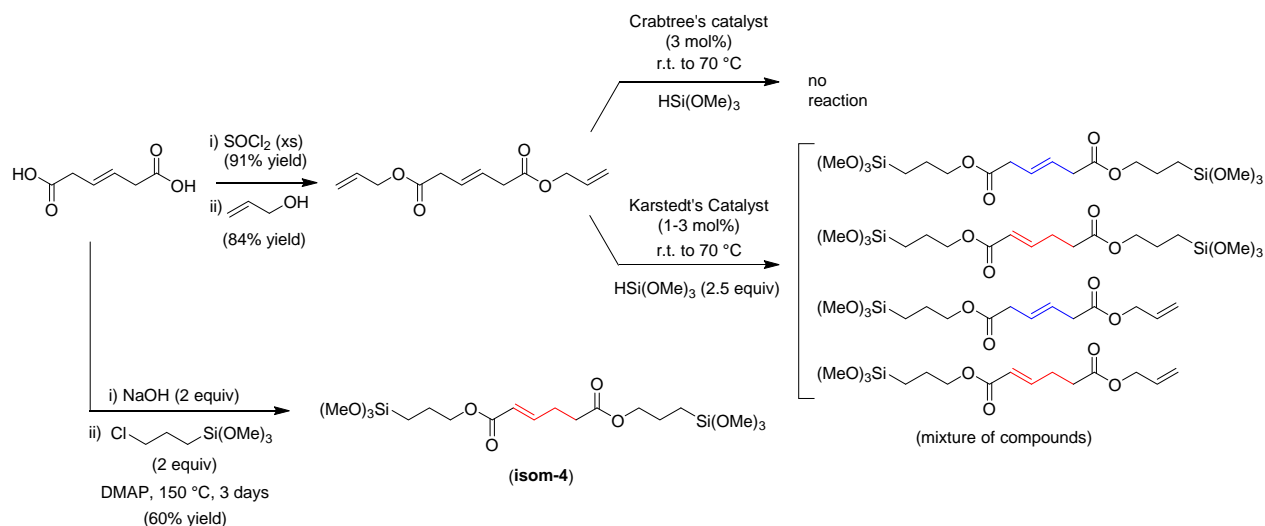


Scheme 2. Ruthenium-catalyzed tandem ROMP/CM of COE in presence of a bis(trialkoxysilyl) functional CTA, showing the two possible polymer types generated (FG: trialkoxysilyl functional group; **DF**: linear α,ω -difunctionalized polymer, **CNF**: cyclic non-functionalized polymer).

Results and Discussion

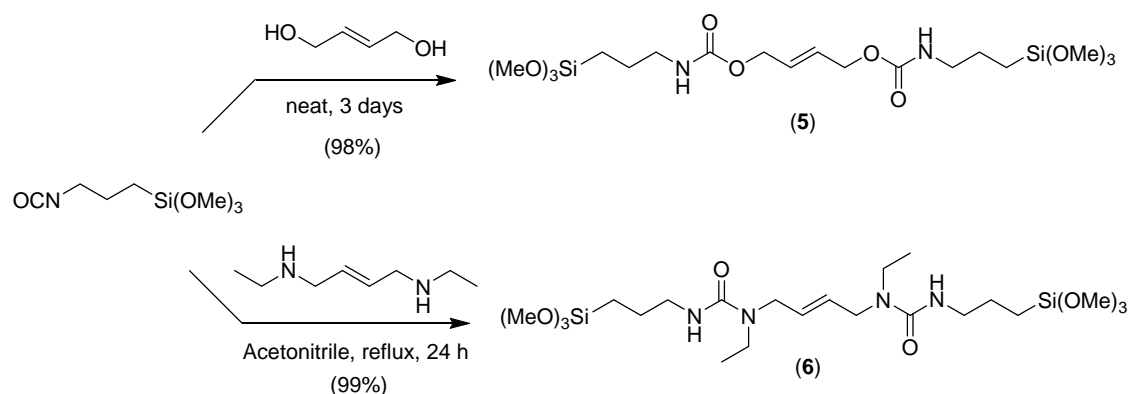
Synthesis of trialkoxysilyl difunctional CTAs. Several bis(trialkoxysilyl) difunctional CTAs (FG–CH=CH–FG) were selected for the present investigation (Scheme 2). Our main objective was to explore the impact of the functionality/spacer adjacent to the metathesis-active C=C moiety onto the overall efficiency of the tandem ROMP/CM process. Hence, in addition to CTA **1** and its bis-homologue **2**,⁴⁹ which do not feature any functional group between the C=C bond and the trialkoxysilyl functions, the fumarate-type CTAs **3-OMe**⁵⁰ and **3-OEt**, the bis-homologue hex-3-enedioate **4**, and diurethane **5** and diurea **6** were targeted to assess electronic effects on the reactivity of the C=C bond, as well as the functional compatibility with the Ru-based catalysts.

The synthesis of bis(3-trimethoxysilylpropyl) *trans*-hex-3-enedioate, CTA **4**, was attempted by hydrosilylation of diallyl *trans*-hex-3-enedioate with trimethoxysilane under a variety of conditions, according to a patent procedure (Scheme 3).⁵¹ However, no reaction was observed using Crabtree's iridium catalyst, whilst mixtures of compounds, with incomplete hydrosilylation and isomerization of the double bond of *trans*-hex-3-enedioate into *trans*-hex-2-enedioate, were systematically recovered with Karstedt's platinum catalyst. Following a similar route as for the synthesis of CTA **3-OEt**, the reaction of disodium hex-3-enedioate with 3-chloropropyltrimethoxysilane in the presence of DMAP, allowed recovering the isomerized form (isom-**4**) of the targeted compound in an overall 60% yield (Scheme 3). Obviously, isomerization of the C=C double bond drives the reaction towards the formation of the conjugated product.



Scheme 3. Attempted synthesis of CTA **4** and isolation of **isom-4**.

The synthesis of diurethane CTA **5** was performed in a straightforward manner *via* addition of 2-butene-1,4-diol onto 3-(trimethoxysilyl)propyl isocyanate in bulk conditions (*i.e.*, neat reagents). Similarly, diurea CTA **6** was recovered in quantitative yield upon reaction of *N,N'*-diethyl-2-butene-1,4-diamine and 3-(trimethoxysilyl)propyl isocyanate (Scheme 4).



Scheme 4. Synthesis of CTA **5** and **6**.

Mechanism and outcome of tandem ROMP/CM process with difunctionalized CTAs.

The polymerization of a cycloolefin promoted by a ruthenium-alkylidene catalyst precursor in

the presence of difunctional CTAs (FG–CH=CH–FG) is assumed to proceed through a tandem one-pot ROMP/CM sequence. Scheme 5 depicts a deliberately simplified possible mechanistic scenario that accounts for the formation of α,ω -bis(trialkoxysilyl) telechelic polycycloolefin (**DF**) along with cyclic non-functionalized polymer (**CNF**), the only two (major and minor, respectively) products observed in this process. It is proposed that the ruthenium-alkylidene precursor **G2** first initiates ROMP (a) that leads to **I** which contains a linear polymer chain, double-bonded to the metal center, with a terminal phenyl group. At this stage, competition shall take place between CM (b) and ring-closure metathesis (RCM) (c), the former functionalization process and the latter backbiting process leading to **III** (with regeneration of alkylidene species **IV**) and **CNF** (along with the Ru-activated linear polymer chain **II** structurally similar to **I**), respectively. Of note, **CNF** may reversibly ring-open (d). Then, **DF** is formed by CM between **III** and **IV** (f).

Supporting this mechanism, the formation of **III** was evidenced by NMR analysis (olefinic signals H⁷, H⁸) of the reaction mixture using a high catalyst loading ([COE]₀/[CTA **2**]₀/[**G2**]₀ = 40:2:1, CH₂Cl₂, 40 °C) (Figure 1; see Figures S17 and S18 in the Supp. Info. for the ¹³C and COSY NMR spectra). The same signals were observed during the ROMP/CM of COE using other CTAs (e.g. alkyl fumarates), indicating that the formation of this species (**III**) is independent of the nature of CTA. Another important observation in support of this mechanism is that, for all ROMP/CM reactions performed in this study, immediately following the addition of the catalyst onto the reagents, a rapid and important increase of the viscosity of the reaction medium was observed; this is consistent with the rapid formation of a high molar mass polymer via ROMP (process (a), refer also to the Experimental section). Then, a gradual decrease of the viscosity occurred, which supports the slower formation of shorter chains via CM with the CTA (process (b)).

Figure 1. ^1H NMR spectrum (400 MHz, CDCl_3 , 298 K) of a crude PCOE sample prepared by ROMP/CM of COE/CTA **2**.

ROMP of COE using different trialkoxysilyl difunctional CTAs and different ruthenium catalysts. To identify and optimize the most efficient catalytic system in terms of selectivity and productivity, the ROMP/CM of COE was investigated using these difunctional CTAs and a series of ruthenium alkylidene catalysts (Scheme 2).

Reactivity of different CTAs using G2 catalyst. The various CTAs were first screened in the ROMP/CM of COE using Grubbs' 2nd generation catalyst (**G2**). For comparison purposes, the reactions were performed under the same model conditions as those used with monofunctional CTAs,³⁰ *i.e.* $[\text{COE}]_0/[\text{CTA}]_0/[\text{G2}]_0 = 2\,000:50\text{--}100:1$ in CH_2Cl_2 at 40 °C. All reactions were at least duplicated and showed a quite good reproducibility of the conversion and molecular data ($\pm 10\%$). Representative results are summarized in Table 1.

Table 1. ROMP/CM of COE catalyzed by **G2** in the presence of various CTAs.^a

Entry	[COE] ₀ (equiv)	CTA	[CTA] ₀ (equiv)	[G2] ₀ (equiv)	Reaction time (h)	COE Conv. ^b (mol%)	CTA Conv. ^b (mol%)	DF + CNF ^c				CNF ^c		
								$M_{n,theo}$ ^d (g.mol ⁻¹)	$M_{n,NMR}$ ^e (g.mol ⁻¹)	$M_{n,SEC}$ ^f (g.mol ⁻¹)	\bar{D}_M ^f	X (wt%)	$M_{n,SEC}$ ^f (g.mol ⁻¹)	\bar{D}_M ^f
1 ⁱ	2000	1	50	1	72	100	0	-	-	-	-	-	-	-
2	2000	2	50	1	24	100	100	4400	5000	8100	1.9	4	13 400	1.2
3	2000	3-OMe	100	1	24	100	19	12 000	12 800	<i>nd</i>	<i>nd</i>	<i>nd</i>	<i>nd</i>	<i>nd</i>
4	2000	3-OMe	100	1	48	100	22	10 000	9700	<i>nd</i>	<i>nd</i>	<i>nd</i>	<i>nd</i>	<i>nd</i>
5	2000	3-OMe	100	1+1 ^g	62	100	32	6800	5700	<i>nd</i>	<i>nd</i>	<i>nd</i>	<i>nd</i>	<i>nd</i>
6	2000	3-OMe	100	1+1+1 ^g	73	100	56	3900	3000	10 300	1.5	13	13 600	1.3
7	2000	3-OEt	100	1	24	100	14	16 000	16 400	20 900	1.7	14	24 000	1.3
8	2000	isom-4	100	1	24	100	60	4200	4000	24 000	1.6	16	28 400	1.4
9	2000	isom-4	100	1+1 ^f	48	100	94	2300	2500	10 700	1.4	14	13 100	1.3
10	2000	5	100	1	24	100	100	2200	2100	4900	1.5	7	8200	1.2
11 ⁱ	2000	6	50	1	72	100	0	-	-	-	-	-	-	-
12 ^h	2000	2	50	1	24	100	100	4400	5100	13 000	1.5	33	17 400	1.3
13 ^h	2000	5	50	1	24	100	100	4400	5900	13 500	1.4	41	18 000	1.2

^a Unless otherwise stated, reactions conducted in CH₂Cl₂ at 40 °C for 24 h (non-optimized reaction time) at 2.5 M. ^b Conversion of COE and CTA as determined by ¹H NMR analysis. ^c **DF** = α,ω -difunctionalized PCOE; **CNF** = cyclic non-functionalized PCOE; $X(\text{CNF})$ (wt%) as determined by column chromatography of the crude polymer (see Experimental Section); $X(\text{DF}) = 100 - X(\text{CNF})$. ^d Theoretical molar mass value of the polymer calculated on the basis of the sole formation of **DF**, from the relation $M_{n,theo} = M_{COE} \times ([COE]_0 \times \text{Conv.}_{COE}) / ([CTA]_0 \times \text{Conv.}_{CTA})$. ^e Experimental molar mass determined by ¹H NMR analysis (refer to the Experimental Section). ^f Number-average molar mass ($M_{n,SEC}$) and dispersity ($\bar{D}_M = M_w/M_n$) values determined by SEC vs. polystyrene standards (uncorrected M_n values) in THF at 30 °C. ^g A second (and a third) equiv of catalyst was added after 24 h (and 24 h). ^h Reactions performed at a lower concentration (0.25 M vs. 2.5 M (entries 1–11)). ⁱ Non-functionalized PCOE (linear **NF** and/or cyclic **NF** PCOE) was the only polymer recovered. *nd*: not determined.

The use of CTA **1** under these conditions led to full conversion of COE but the CTA was not converted at all, and non-functionalized PCOE⁵² was eventually the sole product recovered (Table 1, entry 1). In sharp contrast, when the reaction was performed in the presence of CTA **2**, full conversion of both the monomer and the CTA, with quite selective formation of **DF** PCOE along with minor amounts of **CNF**, was observed (entry 2). In order to explain this striking difference in reactivity between these two CTAs, a control reaction was conducted using a mixture of **1** and **2** (25 + 25 equiv); full conversion of COE and **2**, along with the selective formation of **DF** PCOE terminated only with trimethoxysilylpropenyl groups was then observed, while **1** remained unreacted. This indicates that the **G2** catalyst was not deactivated by possible impurities within **1**, but that the latter CTA is ineffective for CM. This may be tentatively explained by the poor reactivity of putative alkylidene species of the $L_nRu=CHSi(OR)_3$ type as compared to higher $L_nRu=CHCH_2Si(OR)_3$ analogues. In this regard, it is noteworthy to remind that the instability of Ru-alkylidene species $L_nRu=CHR$ bearing α -substituents such as dichlorosilyl, isopropyl and *tert*-butyl, has been reported.^{53,54,55}

With CTAs **3-OMe**, **3-OEt** or **isom-4**, full conversion of COE was observed, yet with a low efficiency of the CM reaction, as evidenced by incomplete conversion of the CTA (entries 3–9). While prolonged reaction times had almost no effect, a higher conversion of CTAs **3** and **isom-4** was achieved upon addition of extra equiv of fresh catalyst over the reaction course. Also, the selectivity was lower as compared to reactions performed with CTA **2**, as ca. 15wt% of **CNF** was systematically formed along **DF**. These observations suggest deactivation of the ruthenium active species, possibly by some impurities within CTAs **3-OMe**, **3-OEt** or **isom-4**.⁵⁶

The ROMP/CM of COE with diurethane **5** proceeded within 24 h with complete monomer and CTA consumption to afford essentially (93wt%) **DF** PCOE (entry 10). Conversely, diurea CTA **6** proved unreactive and only non-functionalized PCOE⁵² was

recovered (entry 11). The inefficiency of CTA **6** may arise from stereoelectronic effects affecting the reactivity of the C=C bond, or from its capacity to inhibit the catalyst for CM due to its basic character.

These results evidence that the nature and purity of the CTAs are key factors for the efficiency of the ROMP/CM process. CTAs **2** and **5** are the most effective ones to access the targeted α,ω -difunctionalized telechelic polyolefins. In light of their ready availability (**2** is synthesized in two steps while **5** is prepared quantitatively by simple addition of neat 2-butene-1,4-diol onto 3-(trimethoxysilyl)propyl isocyanate), these CTAs were selected for the following studies.

It is well known that high dilution conditions favor the intramolecular RCM reaction.^{57,58} In order to better evidence the influence of the concentration on the selectivity of the polymer functionality, highly diluted reactions were performed (entries 12,13). As anticipated, the amount of **CNF** then increased significantly. For instance, using CTA **2**, the amount of **CNF** increased from 4wt% to 33wt% when the concentration decreased from 2.5 M to 0.25 M. Accordingly, to favor the intermolecular CM leading to **DF** PCOE, high concentrations (2.5 M) were systematically used in the present study.

Structure of the polymers. The ¹H NMR spectrum of a representative crude PCOE prepared from CTA **2** at [COE]₀/[**2**]₀/[**G2**]₀ = 2 000:50:1 (Table 1, entry 2) is illustrated in Figure 2. It shows, besides the main chain signals (H⁵-H⁷; note that the repeating COE units in **DF** and **CNF** are indistinguishable), the presence of diagnostic resonances for the trimethoxysilylmethylene end-groups of **DF** PCOE (H¹-H²). The ¹³C{¹H}NMR (Figure 3) and DEPT 135 ¹³C{¹H} NMR spectra (see the Supp. Info., Figure S22) confirmed the presence of these functional groups of **DF**. On the other hand, the ¹H and ¹³C NMR spectra of isolated **CNF** PCOE showed, as anticipated, only the signals for the main chain moieties and no signals for terminal functionalities (see the Supp. Info., Figures S21–S22).

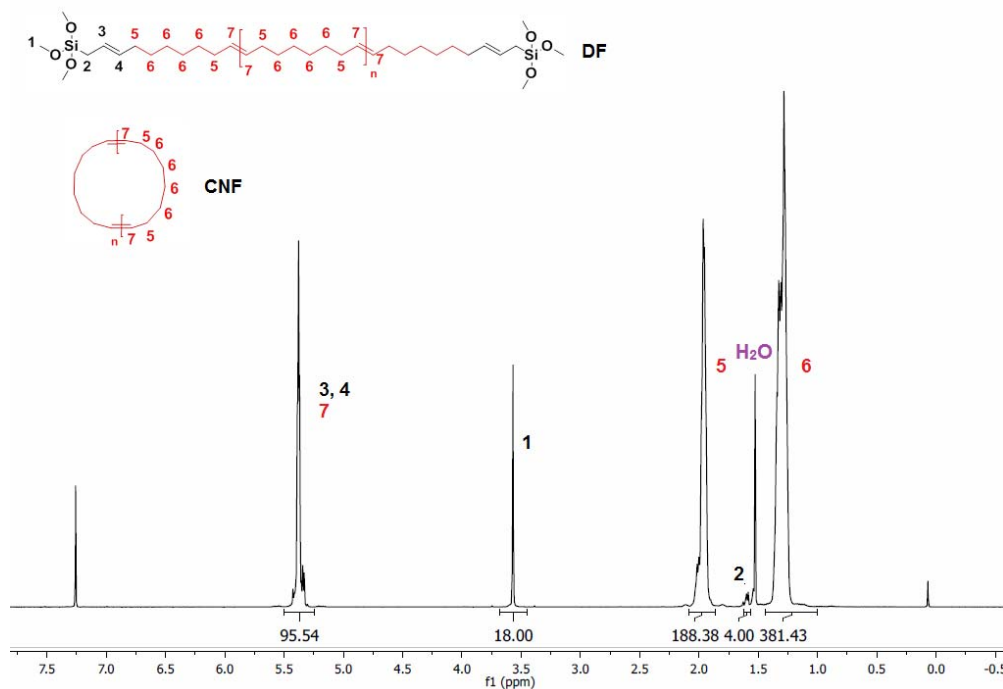


Figure 2. ^1H NMR spectrum (400 MHz, CDCl_3 , 298 K) of a crude PCOE sample prepared by ROMP/CM of COE/CTA **2** (Table 1, entry 2).

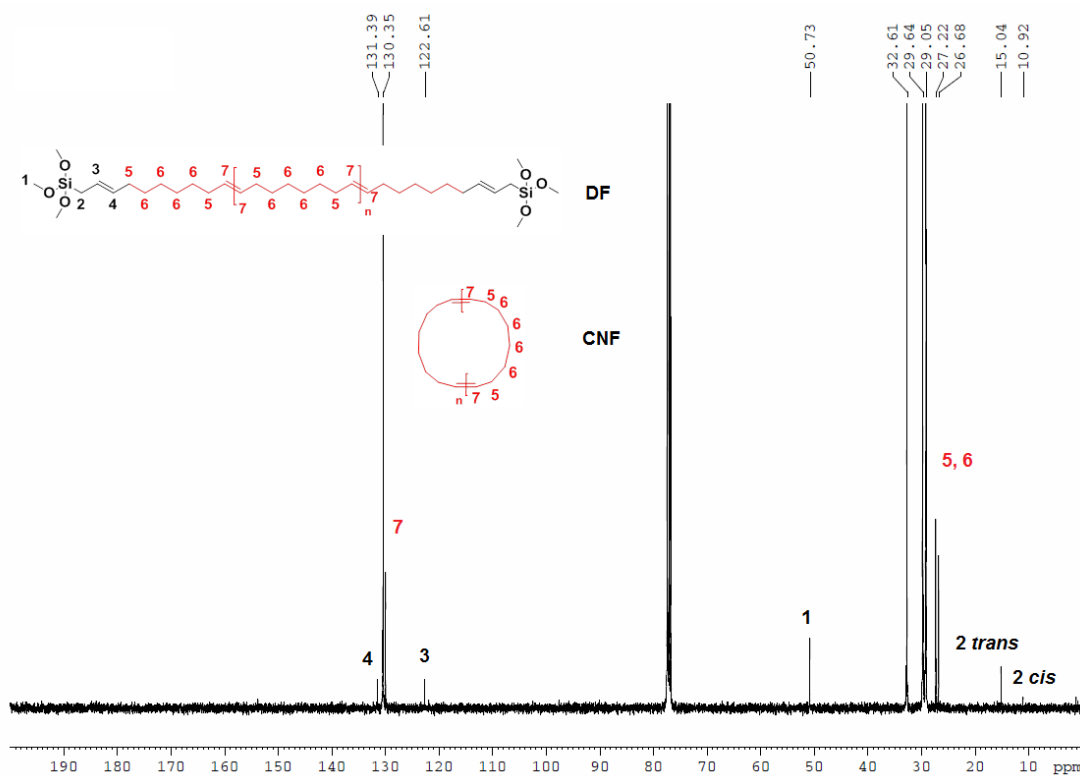


Figure 3. $^{13}\text{C}\{^1\text{H}\}$ NMR spectrum (100 MHz, CDCl_3 , 298 K) of a crude PCOE sample prepared by ROMP-CM of COE/CTA **2** (Table 1, entry 2).

Closer insights into the polymer structure and in the nature of the functional end-groups were gained through MALDI-ToF mass spectrometry. These analyses were performed using either a sodium salt as cationizing agent of functional groups, thereby evidencing only **DF** (see the Supporting Information), or a silver salt as cationizing agent of C=C bonds for the easy detection of both **DF** and **CNF** macromolecules (Figure 4). In fact, in the latter case, two distinct populations were observed: a major one corresponding to **DF** (with *e.g.* $m/z = 1505.9 \text{ g.mol}^{-1}$ for $m = 10$; $m/z_{\text{calcd}} = 1506.1 \text{ g.mol}^{-1}$) and a minor one matching **CNF** (with *e.g.* $m/z = 1430.0 \text{ g.mol}^{-1}$ for $n = 12$; $m/z_{\text{calcd}} = 1430.2 \text{ g.mol}^{-1}$).

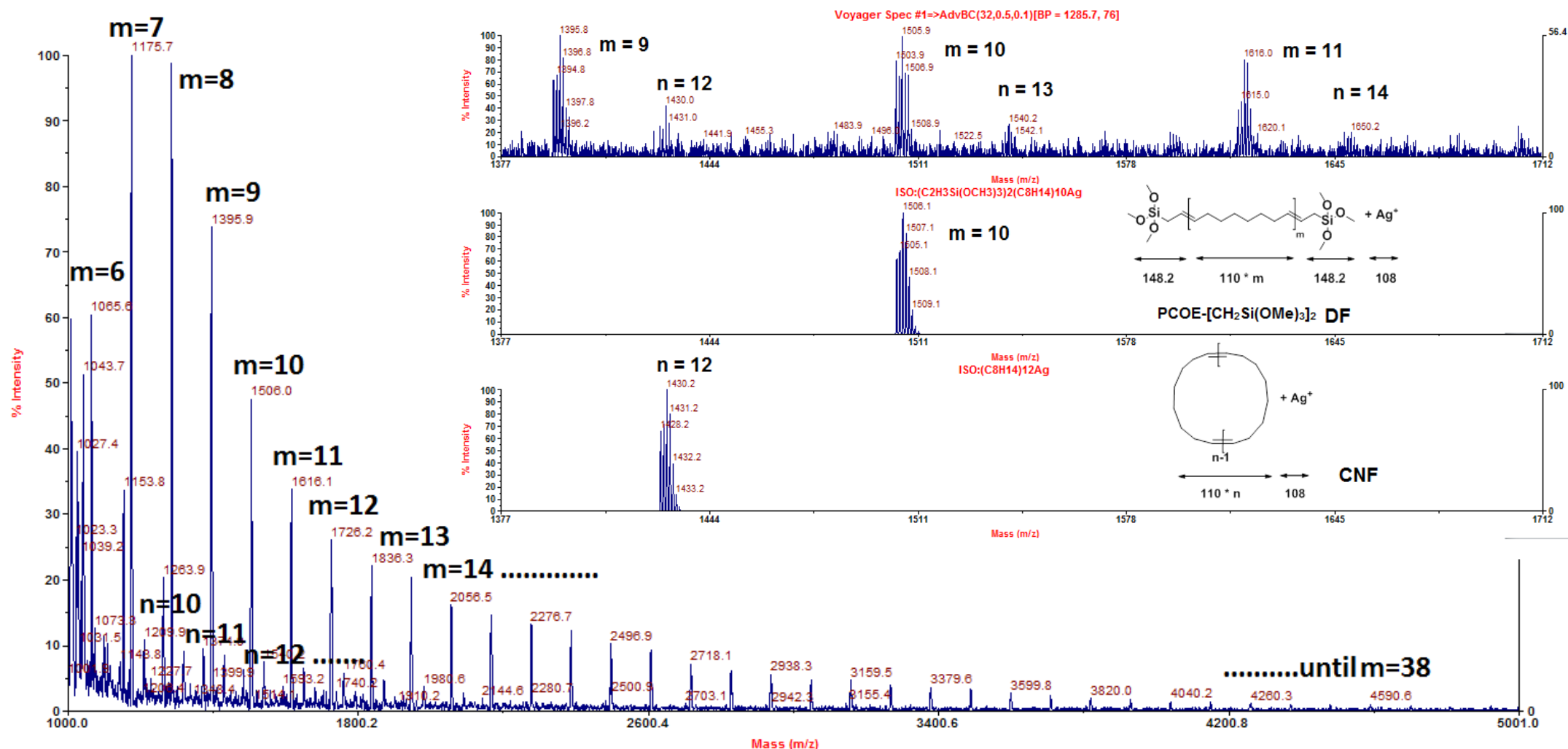


Figure 4. MALDI-ToF mass spectrum (DCTB matrix, AgOCOCF_3) of a crude PCOE sample prepared by ROMP/CM of COE/CTA **2** (Table 1, entry 2), showing a mixture of **DF** and **CNF** PCOE; see top zoomed region and the corresponding middle and bottom simulations for $n = 12$ and $m = 10$, respectively.

The PCOEs obtained using CTA **isom-4** (Table 1, entry 8) were similarly characterized. Their ^1H NMR spectrum (Figure 5) clearly showed the presence of two terminal groups, differing by the position of the C=C bond, due to the dissymmetric structure of the CTA. $^{13}\text{C}\{^1\text{H}\}$ NMR and MALDI-ToF MS data further confirmed the presence of those two different end-groups (see the Supp. Info. Figures S29–S31).

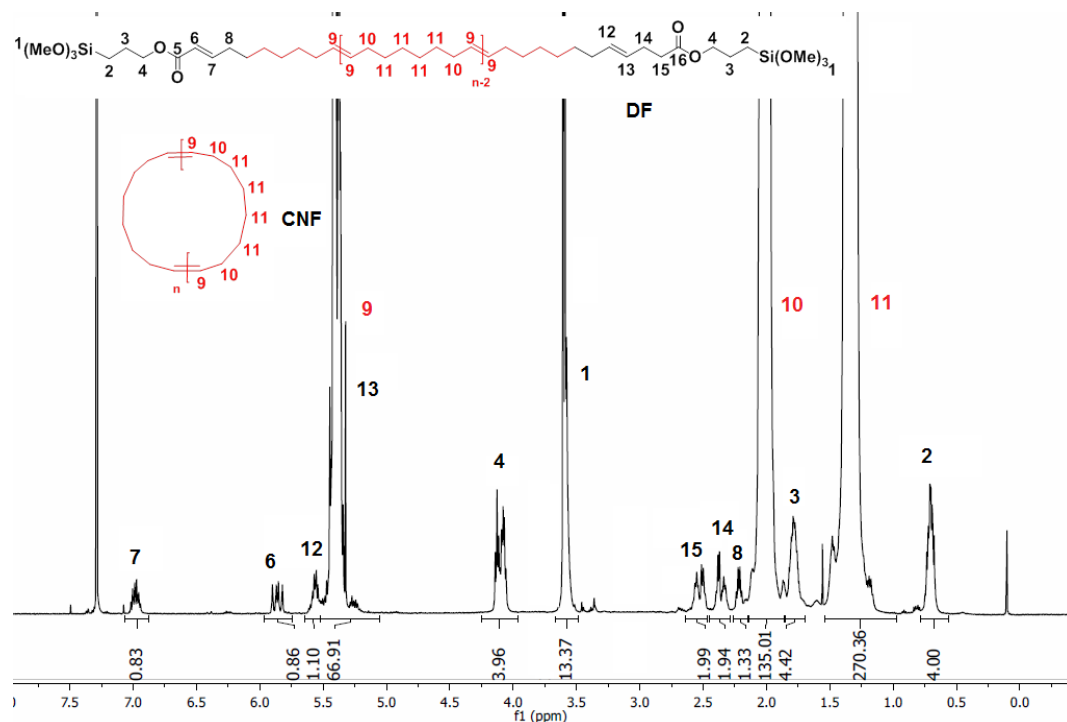


Figure 5. ^1H NMR spectrum (500 MHz, CDCl_3 , 298 K) of a crude PCOE sample prepared by ROMP/CM of COE/CTA **4** using **G2** (Table 1, entry 8). Note that the formula, bearing two different terminal groups, only illustrates one of the three possible ones for **DF**.

The PCOEs obtained using the other CTAs (**3-OMe**, **3-OEt** and **5**) were also characterized by ^1H , $^{13}\text{C}\{^1\text{H}\}$ and ^1H – ^{13}C HMQC NMR, FTIR, ESI and MALDI-ToF MS techniques, which corroborated their chemical structure, and in particular their chain end-groups (See the Supp. Info., Figures S23–S28, S32–36).

Use of different ruthenium catalysts. Obviously, the catalyst is another important parameter to consider in ROMP/CM reactions. Hence, in addition to Grubbs' 2nd generation catalyst (**G2**), the efficiency of Grubbs' 3rd generation catalyst (**G3**),⁵⁹ Hoveyda-Grubbs's (**HG2**),⁶⁰ Zhan's (**Zhan**),⁶¹ and of some OmegaCat catalysts (**M73-SiMes**, **M73-SiPr**)⁶² (Figure 6), was compared in the ROMP/CM of COE using CTAs **2** and **5**. Representative results (also from at least duplicated experiments) are summarized in Table 2. The influence of the solvent has been evidenced previously in ROMP/CM reactions using monofunctional CTAs.^{30,63} For the present reactions with difunctional CTAs, CH₂Cl₂ was also found to be the best solvent in terms of catalytic productivity and selectivity. Reactions performed in toluene showed systematically lower conversions; see for instance Table 2, entry 23.

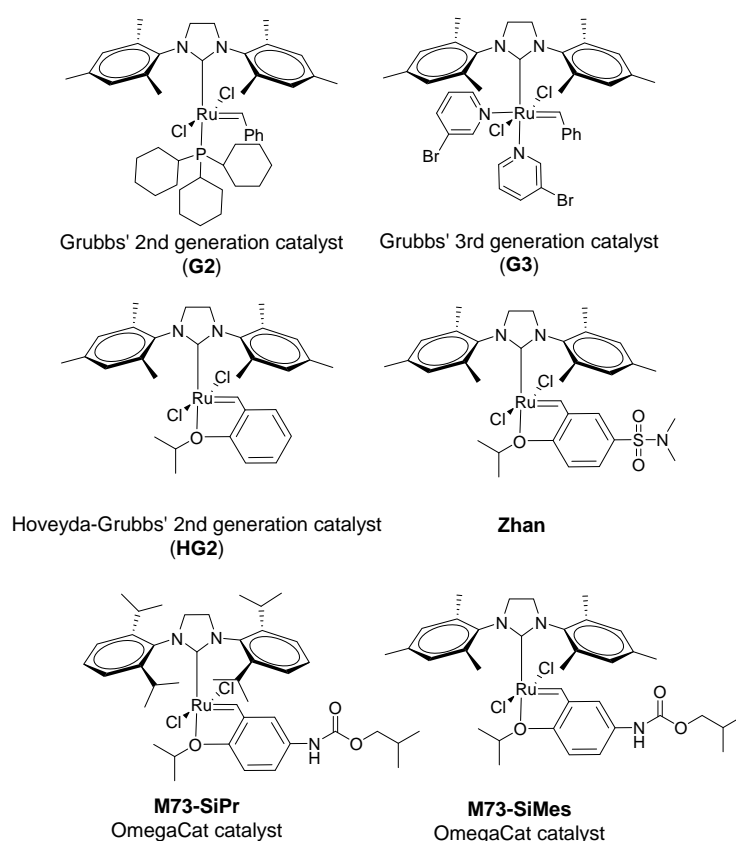


Figure 6. Olefin metathesis Ru-catalysts screened in this study.

Table 2. ROMP/CM of COE/CTAs with various ruthenium catalysts.^a

Entry	[COE] ₀ (equiv)	CTA	[CTA] ₀ (equiv)	[Ru] (1 equiv)	COE Conv. ^b (mol%)	CTA Conv. ^b (mol%)	DF + CNF ^c				CNF		
							$M_{n,theo}$ ^d (g.mol ⁻¹)	$M_{n,NMR}$ ^e (g.mol ⁻¹)	$M_{n,SEC}$ ^f (g.mol ⁻¹)	D_M ^f	X^c (wt%)	$M_{n,SEC}$ ^f (g.mol ⁻¹)	D_M ^f
1	2000	2	50	G2	100	100	4400	5400	8100	1.5	4	13 400	1.2
2	2000	2	50	G3	100	100	4400	4900	8100	1.4	5	15 100	1.2
3	2000	2	50	HG2	100	100	4400	5100	8500	1.6	3	11 200	1.3
4	2000	2	50	Zhan	100	100	4400	5100	7900	1.4	7	13 000	1.3
5	2000	2	50	M7₃-SIPr	100	100	4400	6400	14 600	1.6	11	28 100	1.2
6	2000	2	50	M7₃-SIMes	100	100	4400	5600	14 000	1.8	9	23 600	1.2
7	8000	2	200	G2	100	100	4400	5000	7600	1.7	8	15 300	1.3
9	16 000	2	400	G2	100	100	4400	4800	12 300	1.8	11	23 600	1.3
10	48 000	2	800	G2	100	100	6600	6400	24 000	1.6	12	35 000	1.2
11	48 000	2	800	G3	100	100	4400	4800	29 200	1.7	14	45 000	1.4
12	48 000	2	800	HG2	100	100	6600	7200	39 500	2.0	16	46 000	1.4
13	48 000	2	800	Zhan	100	100	6600	6700	74 500	1.8	21	77 000	1.5
14	48 000	2	800	M7₃-SIPr	100	100	6600	8900	104 000	2.0	27	136 000	1.7
15	48 000	2	800	M7₃-SIMes	100	100	6600	9200	40 000	1.8	23	50 000	1.4
16	50 000	5	1250	G2	100	100	4400	4600	34 000	1.5	8	60 000	1.2
17 ^g	50 000	5^g	1250	G2	100	100	4400	5100	16 000	2.0	10	31 000	1.3
18	50 000	5	1250	HG2	100	100	4400	5400	17 700	1.5	18	34 200	1.3
19	50 000	5	1250	G3	100	100	4400	5100	21 600	1.7	13	45 400	1.5
20	100 000	5	5000	G2	86	100	1900	2400	25 400	2.0	36	50 000	1.4
21	100 000	5	5000	HG2	95	100	2100	2100	19 400	1.6	21	54 700	1.3
22	100 000	5	5000	G3	53	0	-	-	<i>nd</i>	<i>nd</i>	100	<i>nd</i>	<i>nd</i>
23 ^h	100 000	5	5000	G2	51	0	-	-	<i>nd</i>	<i>nd</i>	100	<i>nd</i>	<i>nd</i>

^a Unless otherwise stated, reactions conducted in CH₂Cl₂ at 40 °C for 24 h (non-optimized reaction time) at 2.5 M. ^b Conversion of COE and CTA as determined by ¹H NMR analysis. ^c **DF** = α,ω-difunctionalized PCOE; **CNF** = cyclic non-functionalized PCOE; $X(\text{CNF})$ (wt%) as determined by column chromatography of the crude polymer (see Experimental Section); $X(\text{DF}) = 100 - X(\text{CNF})$. ^d Theoretical molar mass value of the polymer calculated from $M_{n,theo} = M_{COE} \times ([COE]_0 \times \text{Conv.}_{COE}) / ([CTA]_0 \times \text{Conv.}_{CTA})$, on the basis of the formation of only **DF**, *i.e.* without taking into account any **CNF**. ^e Experimental molar mass value determined by ¹H NMR analysis (see Experimental Section). ^f Number-average molar mass ($M_{n,SEC}$) and dispersity ($D_M = M_w/M_n$) values determined by SEC vs. polystyrene standards (uncorrected M_n values) in THF at 30 °C. ^g Synthesis of CTA **5** and ROMP/CM of COE conducted in one-pot (Scheme 6). ^h Reaction performed in toluene.

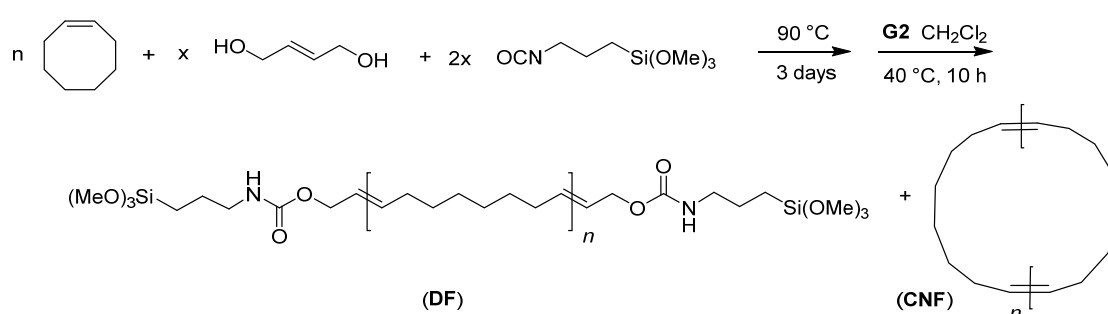
Productivity of the catalysts. Using CTA **2** under our standard conditions, the formation of **DF** PCOE along with minor amounts of **CNF** PCOE (*vide infra*) was observed with all ruthenium catalysts (Table 2, entries 1–6). Increasing the COE and CTA **2** loading up to 48 000 and 800 equiv, respectively, confirmed a high productivity of all ruthenium catalysts with effective turnover numbers (TONs) up to 48 000 (Table 2, entries 7–15).

Full conversion of the reagents was also observed using CTA **5** with **G2**, **G3** and **HG2** catalysts at $[\text{COE}]_0/[\mathbf{5}]_0/[\text{Ru}]_0 = 50\,000:1\,250:1$ (entries 16–19). Further increasing the monomer and CTA loads to 100 000 and 5 000 equiv, respectively, enabled differentiating the ultimate abilities of these catalysts. **G2** gave 86mol% conversion of COE, while 95mol% conversion was reached with **HG2**, both with full conversion of the CTA (entries 20, 21). On the other hand, **G3** led to only 50mol% of conversion of COE and no conversion of the CTA under these conditions (entry 22).

DF/CNF Selectivity of the catalysts. The amount of **CNF** PCOE in the crude polymer sample was quantified after trapping the **DF** polymer onto acidified silica. With CTA **2**, at relatively low reagent loadings ($[\text{COE}]_0/[\mathbf{2}]_0/[\text{Ru}]_0 = 2\,000:50:1$), the mixture of polymers obtained from all the ruthenium catalysts contained 89–97wt% of **DF**; catalysts **G2**, **G3**, **HG2** and Zhan's were more selective (93–97wt% **DF**) than those from OmegaCat (89–91wt% **DF**) (entries 1–6). Larger amounts of **CNF** PCOE (8–27wt%) were recovered at higher reagent loads. This probably reflects partial catalyst decay under such demanding conditions, and the difficulty to complete CM.

The same trends were observed with CTA **5**: at $[\text{COE}]_0/[\mathbf{5}]_0/[\text{Ru}]_0 = 50\,000:1\,250:1$ with **G2**, **HG2** and **G3** catalysts, the amount of **CNF** remained low (8–18wt%) (entries 16–19). With a monomer and CTA load of 100 000 and 5 000 equiv, respectively, the amount of **CNF** increased up to 36wt% with **G2** catalyst but remained at a reasonable 21wt% with **HG2** (entries 20, 21). Overall, these data indicated that **HG2** is the most productive (robust) and selective out of the different catalysts investigated for this process.

Interestingly, the reaction with **5** could be performed in a simple one-pot protocol, by generating the latter CTA *in situ* (Scheme 6). Hence, COE, 2-butene-1,4-diol and 3-(trimethoxysilyl)propyl isocyanate were placed in a flask at 90 °C for 72 h under neat conditions to generate CTA **5**. Then, the reaction mixture was cooled to 40 °C and a solution of **G2** in CH₂Cl₂ was added in to promote the ROMP/CM process. This reaction protocol advantageously led to the same results as the reactions carried out with prior isolation of CTA **5** (entries 16 vs. 17).



Scheme 6. Tandem ROMP/CM of COE/**5** catalyzed by **G2** catalyst using a one-pot protocol including the *in situ* generation of CTA **5** (Table 2, entry 17).

Molar masses of the polymers. The $M_{n,\text{NMR}}$ values were determined from the integral ratio of the signals of end-groups' hydrogens to the internal olefin hydrogens (*vide supra*, Figures 1 and 4). The $M_{n,\text{NMR}}$ values of all polymers matched quite well the theoretical molar mass values (calculated without taking into account any **CNF**, a reasonable hypothesis considering the actual low amounts) (Tables 1 and 2). The dispersity of the crude polymers were all monomodal and moderately large ($D_M = 1.4\text{--}2.0$), as classically reported for ROMP/CM reactions.^{40,64,65} The uncorrected $M_{n,\text{SEC}}$ values of the **DF** polymers were always higher than the corresponding $M_{n,\text{NMR}}$ and $M_{n,\text{theo}}$ values; this most likely arises from their different hydrodynamic volumes as compared to polystyrene standards used for calibration. On the other hand, the difference between the $M_{n,\text{SEC}}$ and the corresponding $M_{n,\text{NMR}}$ values is much

more significant for polymers recovered from reactions performed at higher monomer loadings (> 5000 equiv), although the same final M_n value was targeted. We noted also that the $M_{n,SEC}$ values slightly decrease by adding more catalyst: in a reaction performed at $[COE]_0/[5]_0/[G2]_0 = 50\,000:1\,250:1$, the $M_{n,SEC}$ value of the crude polymer (93wt% **DF**) observed after 24 h decreased from 26 500 down to 20 100 and 17 400 g.mol⁻¹ ($D_M = 1.4$ for all) upon adding, a second (after 24 h) and a third (after 48 h) equiv of **G2** catalyst, respectively. These observations suggest that, in reactions carried out at high reagent loadings, the CM process does not reach equilibrium (due to low amounts of active Ru species), leaving some macromolecules of high molar mass that are detected in SEC analysis (but not in NMR that simply provides an average M_n value without dispersity information).

Conclusions

The ROMP/CM of COE with several bis(trialkoxysilyl) difunctional alkenes as CTAs in the presence of Ru-alkylidene catalysts offers an effective access to well-defined α,ω -bis(trialkoxysilyl) telechelic PCOEs (**DF**). The only side-product is the cyclic non-functional PCOE (**CNF**), which is always formed in minor quantities (typically 10–20wt%). The use of such difunctional CTAs is much more selective than that of monofunctional analogues, such as trialkoxysilyl acrylates, which lead to a structural diversity of polyolefins out of which **DF** is a minor component.³⁰

The productivity and selectivity of the catalytic process depend much on the nature of the CTA and catalyst. Out of the six CTAs investigated, **2** and **5** allowed a high productivity with remarkable turnover numbers up to 95 000 mol(COE).mol(Ru)⁻¹ and 5 000 mol(CTA).mol(Ru)⁻¹; CTA **5** is easy to prepare, and can even be conveniently generated *in situ* in the one-pot ROMP/CM. In contrast, **3-OMe**, **3-OEt**, **4** and **6** proved ineffective, since, in their presence, the **G2** catalyst most likely deactivated before the CM process was completed; it is still unclear whether this deactivation is inherent to the structure of these

CTAs (and of the corresponding Ru-alkylidene species derived thereof) or from the presence of unidentified residual impurities. **G2** and **HG2** were found to be the most productive and selective catalysts, in light of their high TONs and low amounts of **CNF** polymer formed.

All of these features allow envisaging the industrial production of trialkoxysilyl difunctionalized polyolefins. The trialkoxysilyl groups can be engaged in crosslinking reactions under the action of moisture to form siloxanes, which ensure good sealing properties. Preliminary investigations show that the rate of crosslinking of these **DF** PCOE is twice higher than that of the corresponding monofunctionalized polymers. Also, the viscosity of the **DF** materials can be controlled by adjusting the nature of the main chain segments, notably by copolymerizing instead of homopolymerizing cycloolefins. Detailed results along these lines will be reported in due course.

Experimental Section

Materials. All catalytic experiments were performed under inert atmosphere (argon, < 3 ppm O₂) using standard Schlenk line and glove box techniques. Cyclooctene (COE) and CH₂Cl₂ (stabilized with amylene) were dried and distilled over CaH₂ before use. Grubbs' 2nd-generation catalyst (**G2**), Grubbs' 3rd generation catalyst (**G3**), Hoveyda-Grubbs' 2nd generation catalyst (**HG2**), Zhan's catalyst (**Zhan**) were purchased from Sigma-Aldrich and used as received. Catalysts **M7₃-SIMes** and **M7₃-SIPr** were provided by OmegaCat Co. and used as received. 1,2-Bis(triethoxysilyl)ethene (**1**; Aldrich) and bis(3-trimethoxysilylpropyl) fumarate (**3-OMe**, Gelest) were purchased and used as received. CTAs **2**⁴⁹ (Figures S1–S2) and **3-OEt**⁵⁰ (Figures S3–S4) were synthesized according to the reported literature procedures.

Instrumentation and measurements. ¹H (500, 400 MHz) and ¹³C{¹H} (125, 100 MHz) NMR spectra were recorded on Bruker Avance AM 500 and AM 400 spectrometers at 23 °C in CDCl₃. Chemical shifts (δ) are reported in ppm and were referenced internally relative to

tetramethylsilane (δ 0 ppm) using the residual ^1H and ^{13}C solvent resonances. A relaxation delay of 1 s and 1.5 s was used during the acquisition to afford “quantitative” ^1H and $^{13}\text{C}\{^1\text{H}\}$ NMR spectra, respectively.

Monomer conversions were determined from ^1H NMR spectra of the crude polymer sample, from the integration (Int.) ratio $\text{Int.}_{\text{Polymer}}/[\text{Int.}_{\text{Polymer}} + \text{Int.}_{\text{monomer}}]$, using the methine hydrogens ($-\text{CH}=\text{CH}-$: δ 5.30 ppm for PCOE, and 5.66 ppm for COE).

The molar mass values of the polymers samples were determined by ^1H NMR analysis in CDCl_3 ($M_{n,\text{NMR}}$) from the integral ratio of the signals of end-groups hydrogens (typically δ 3.56 (H^1)) to internal olefin hydrogens (δ 5.38 (H^7)) (see Figure 4).

The average molar mass ($M_{n,\text{SEC}}$) and dispersity ($D_M = M_w/M_n$) values were determined by size exclusion chromatography (SEC) in THF at 30 °C (flow rate = 1.0 $\text{mL}\cdot\text{min}^{-1}$) on a Polymer Laboratories PL50 apparatus equipped with a refractive index detector and a set of two ResiPore PLgel 3 μm MIXED-E 300×7.5 mm columns. The polymer samples were dissolved in THF (2 $\text{mg}\cdot\text{mL}^{-1}$). All elution curves were calibrated with 12 monodisperse polystyrene standards (M_n range = 580–380,000 $\text{g}\cdot\text{mol}^{-1}$). $M_{n,\text{SEC}}$ values of polymers were uncorrected for their possible difference in hydrodynamic volume vs. polystyrene. The SEC traces of the polymers all exhibited a monomodal and symmetrical peak.

FTIR spectra were recorded on a IR Affinity-1 SHIMADZU spectrometer equipped with a PIKE technologies GladiATR device for measurements.

MALDI-ToF mass spectra were recorded at the CESAMO (Bordeaux, France) on a Voyager mass spectrometer (Applied Biosystems) equipped with a pulsed N_2 laser source (337 nm, 4 ns pulse width) and a time-delayed extracted ion source. Spectra were recorded in the positive-ion mode using the reflectron mode and with an accelerating voltage of 20 kV. A freshly prepared solution of the polymer sample in THF (HPLC grade, 10 $\text{mg}\cdot\text{mL}^{-1}$), a saturated solution of *trans*-2-[3-(4-*tert*-butylphenyl)-2-methyl-2-propenylidene]malononitrile

(DCTB, 10 mg) in THF (1 mL, HPLC grade) were prepared. A MeOH solution of the cationisation agent (NaI or AgTFA, 10 mg.mL⁻¹) was also prepared. The solutions were combined in a 10:1:1 v/v of matrix-to-sample-to-cationisation agent. 1–2 µL of the resulting solution were deposited onto the sample target and vacuum-dried.

HRMS data were recorded with a Bruker MicrOTOF-Q II mass spectrometer equipped with an ESI (Electrospray Ionization) source in the positive mode. The acceleration voltage was 4–5 kV.

Synthesis of CTA isom-4. A 100 mL round-bottom flask, equipped with a magnetic stir bar, was charged with *trans*-3-hexenedioic acid (2.00 g, 13.9 mmol), NaOH (1.11 g, 27.8 mmol) and distilled water (10.0 mL). The mixture was placed at 40 °C for 10 h. Disodium *trans*-3-hexenedioate (2.60 g) was obtained as a white powder upon removing water under vacuum. Under argon atmosphere, a 100 mL round-bottom Schlenk flask, equipped with a magnetic stir bar, was charged with 3-chloropropyltrimethoxysilane (5.52 g, 5.2 mL, 27.8 mmol). Disodium *trans*-3-hexenedioate (2.60 g, 13.8 mmol) and DMAP (68 mg, 0.56 mmol) were then added into the stirred mixture. Once the addition was completed, the reaction mixture was heated to 150 °C for 3 days. The reaction was then cooled to 50 °C. At this temperature, petroleum ether (15 mL) was added. After 10 min of stirring, the precipitate was filtered off. The yellow liquid recovered was placed under vacuum to give the desired compound 3.30 g (51% yield). ¹H NMR (500 MHz, CDCl₃, 298 K): δ 0.67 (m, 4H, CH₂CH₂Si), 1.76 (m, 4H, CH₂CH₂Si), 2.50 (m, 4H, =CHCH₂CH₂CO), 3.59 (s, 18H, SiOCH₃), 4.07 (m, 4H, CH₂CH₂OCO), 5.85 (d, *J* = 16 Hz, 1H, OCOCH=CH), 6.93 (m, 1H, OCOCH=CH) (Figure S5). ¹³C{¹H} NMR (125 MHz, CDCl₃, 298 K): δ 5.2 (CH₂CH₂Si), 21.9 (CH₂CH₂Si), 27.1 (=CHCH₂CH₂CO), 32.3 (=CHCH₂CH₂CO), 50.1 (SiOCH₃), 66.3 (CH₂CH₂OCO), 121.9 (OCOCH=CH), 146.5 (OCOCH=CH), 166.0 (OCOCH=CH), 171.9 (CH₂COOCH₂) (Figure S6). ESI-HRMS: [M+Na]⁺ (C₁₈H₃₆O₁₀NaSi₂) calcd (g.mol⁻¹):

491.1745, found: 491.1739 (Figure S7). FTIR (cm^{-1}): ν 2943 (C–H); 2841 (C–H); 1720.50 (C=O); 1263 (C–O); 1188 (Si–O–C); 1074 (C–H); 776 (Si–O–C) (Figure S8).

Synthesis of CTA 5. Under argon atmosphere, a 50 mL round-bottom Schlenk flask equipped with a magnetic stir bar, was charged sequentially with 2-butene-1,4-diol (2.1 g, 2.0 mL, 24.3 mmol) and 3-(trimethoxysilyl)propyl isocyanate (10.3 g, 9.6 mL, 50.0 mmol). The reaction mixture was placed at 80 °C for 3 days. The desired product was obtained as a yellow oil (11.8 g, 98% yield). ^1H NMR (500 MHz, CDCl_3 , 298 K): δ 0.47 (d, J = 8.6 Hz, 4H, $\text{CH}_2\text{CH}_2\text{Si}$), 1.44 (m, 4H, $\text{CH}_2\text{CH}_2\text{Si}$), 2.98 (m, 4H, $\text{CH}_2\text{CH}_2\text{NHCO}$), 3.39 (s, 18H, SiOCH_3), 4.47 (s, 4H, $\text{CH}=\text{CHCH}_2\text{O}$), 5.53 (m, 2H, $\text{CH}=\text{CH}$) (Figure S9). $^{13}\text{C}\{^1\text{H}\}$ NMR (125 MHz, CDCl_3 , 298 K): δ 6.1 ($\text{CH}_2\text{CH}_2\text{Si}$), 22.9 ($\text{CH}_2\text{CH}_2\text{Si}$), 43.2 ($\text{CH}_2\text{CH}_2\text{NHCO}$), 50.3 (SiOCH_3), 60.0 ($\text{CH}=\text{CHCH}_2\text{O}$), 128.1 ($\text{CH}=\text{CH}$), 156.2 (OCONH) (Figure S10). ESI-HRMS: $[\text{M}+\text{Na}]^+$ ($\text{C}_{18}\text{H}_{32}\text{N}_2\text{O}_{10}\text{NaSi}_2$) calcd ($\text{g}\cdot\text{mol}^{-1}$): 521.1963, found: 521.1968 (Figure S11). FTIR (cm^{-1}): ν 3337 (N–H); 2941.44 (C–H); 2841 (C–H); 1697.36 (C=O); 1526 (C–N); 1238 (C–O); 1072 (Si–O–C); 988 (C–H); 773 (Si–O–C) (Figure S12).

Synthesis of CTA 6. Under argon atmosphere, a 50 mL round-bottom Schlenk flask, equipped with a magnetic stir bar, was charged sequentially with *N,N'*-diethyl-2-butene-1,4-diamine (421 mg, 0.5 mL, 3.0 mmol) and 3-(trimethoxysilyl)propyl isocyanate (1.21 g, 1.1 mL, 6.0 mmol). The reaction mixture was placed at 80 °C for 3 days. The desired product was obtained as a yellow oil (1.60 g, 99% yield). ^1H NMR (500 MHz, CDCl_3 , 298 K): δ 0.59 (t, J = 8.4 Hz, 4H, $\text{CH}_2\text{CH}_2\text{Si}$), 1.05 (t, J = 7.1 Hz, 6H, NCH_2CH_3), 1.54 (m, 4H, $\text{CH}_2\text{CH}_2\text{Si}$), 3.16 (m, 4H, $\text{CH}_2\text{CH}_2\text{NHCO}$, 4H, NCH_2CH_3), 3.50 (s, 18H, SiOCH_3), 3.77 (s, 4H, $\text{CH}=\text{CHCH}_2$), 4.56 (t, J = 5.8 Hz, 2H, *NH*), 5.52 (s, 2H, $\text{CH}=\text{CH}$) (Figure S13). $^{13}\text{C}\{^1\text{H}\}$ NMR (125 MHz, CDCl_3 , 298 K): δ 1.8 (NCH_2CH_3), 6.4 ($\text{CH}_2\text{CH}_2\text{Si}$), 13.5 ($\text{CH}_2\text{CH}_2\text{Si}$), 41.3 ($\text{CH}_2\text{CH}_2\text{NHCO}$), 43.1 (NCH_2CH_3), 47.8 ($\text{CH}=\text{CHCH}_2\text{N}$), 50.5 (SiOCH_3), 128.5 ($\text{CH}=\text{CH}$), 157.5 (CO) (Figure S14). ESI-HRMS: $[\text{M}+\text{Na}]^+$ ($\text{C}_{18}\text{H}_{32}\text{N}_2\text{O}_{10}\text{NaSi}_2$), calcd ($\text{g}\cdot\text{mol}^{-1}$): 575.2908, found: 575.2908 (Figure S15). FTIR (cm^{-1}): ν 3346 (N–H); 2939.52 (C–H); 2839

(C–H); 1624 (C=O); 1526 (C–N); 1279 (C–O); 1074 (Si–O–C); 972 (C–H); 766 (Si–O–C) (Figure S16).

General ROMP Procedure. All polymerizations were performed according to the following typical procedure (Table 1, entry 1). The only differences lie in the nature of the solvent, catalyst, CTA and its initial concentration ($[\text{COE}]_0$ and $[\text{CTA}]_0$). Under argon atmosphere, a 20 mL Schlenk flask, equipped with a magnetic stir bar, was charged sequentially with dry CH_2Cl_2 (5.0 mL), COE (1.56 mL, 1.32 g, 12.0 mmol) and CTA **2** (89 mg, 0.30 mmol). The resulting solution was placed at 40 °C and the polymerization was started upon addition, *via* a cannula, of a dry, freshly prepared CH_2Cl_2 solution (2.0 mL) of **G2** (5.0 mg, 5.3 μmol). The reaction mixture turned highly viscous within 2 min. The viscosity then slowly decreased over the next 10 min. After the desired reaction time (typically 24 h), volatiles were removed under vacuum. The polymer was then recovered upon precipitation in excess methanol (50 mL), thereby allowing removal of the catalyst residues, filtration and drying at 25 °C under vacuum (95% yield). All polymers were recovered as white powders, readily soluble in chloroform and THF, and insoluble in methanol (Tables 1 and 2).

Separation of cyclic non-functionalized (CNF) polymers from functionalized polymers. CNF PCOE was separated from crude polymers by column chromatography on silica gel 60 acidified with HCl (37%) until $\text{pH} < 2$, using CH_2Cl_2 as eluent. Functionalized polymers (**DF**) thus remained grafted onto the acidified silica, while **CNF** PCOEs were isolated from the eluted solution.

Acknowledgements

Financial support of this research by Bostik and Total Cies (Ph.D. grant to X.M.) is gratefully acknowledged. OmegaCat Company is gratefully acknowledged for providing **M7₃-SIMes** and **M7₃-SIPr** catalysts.

Supporting information includes ^1H and $^{13}\text{C}\{^1\text{H}\}$ NMR spectra, FTIR spectra, mass spectra as well as SEC traces of CTAs, and representative PCOE samples.

References and Notes

- ¹ T. W. Greenle, *Adhesion Science and Technology, A*, 1975, 339 (H. L. Lee Plenum, New York).
- ² Y. Nomura, A. Sato, S. Sato, H. Mori and T. Endo, *J. Polym. Sci. A: Polym. Chem.*, 2007, **45**, 2689-2704.
- ³ A. Hirao, T. Hatayama, T. Nagawa, M. Yamaguchi, K. Yamaguchi and S. Nakahama, *Macromolecules*, 1987, **20**, 242-247.
- ⁴ A. Hirao, T. Nagawa, T. Hatayama, K. Yamaguchi and S. Nakahama, *Macromolecules*, 1985, **18**, 2101-2105.
- ⁵ K. Tekenaka, A. Hirao, T. Hattori and S. Nakahama, *Macromolecules*, 1987, **20**, 2035-2037.
- ⁶ K. Tekenaka, A. Hirao, T. Hattori and S. Nakahama, *Macromolecules*, 1989, **22**, 1563-1567.
- ⁷ K. Tekenaka, K. Kato, A. Hirao, T. Hattori and S. Nakahama, *Macromolecules*, 1990, **23**, 3619-3625.
- ⁸ H. Ozaki, A. Hirao and S. Nakahama, *Macromolecules*, 1992, **25**, 1391-1395.
- ⁹ M. Kobayashi, T. Chiba, K. Tsuda and M. Takeishi, *J. Polym. Sci. A: Polym. Chem.*, 2005, **43**, 2754-2764.
- ¹⁰ A. Hirao and S. Nakahama, *Prog. Polym. Sci.*, 1992, **17**, 283-317.
- ¹¹ W. E. Lindsell, K. Radha and I. Soutar, *Polym. Int.*, 1991, **25**, 1-6.
- ¹² A. K. Roy, Dow Corning Corp., *US Pat.* 5,561,210, 1996.
- ¹³ D. Derouet, S. Forgeard and J.-C. Brosse, *Macromol. Chem. Phys.*, 1998, **199**, 1835-1842.
- ¹⁴ D. Derouet, S. Forgeard and J.-C. Brosse, *Macromol. Chem. Phys.*, 1999, **200**, 10-24.
- ¹⁵ C.-W. Lee, S.-W. Joo and M.-S. Gong, *Sens. Actuat., B*, 2005, **105**, 150-158.
- ¹⁶ F. Schapman, J. P. Couvercelle and C. Bunel, *Polymer*, 1998, **39** (20), 4955-4962.
- ¹⁷ K. Takenaka, A. Hirao and S. Nakahama, *Makromol. Chem.*, 1992, **193**, 1943-1953.
- ¹⁸ K. Takenaka, S. Kawamoto, M. Miya, H. Takeshita and T. Shiomi, *Polym. Int.*, 2010, **59**, 891-895.
- ¹⁹ B. P. S. Chauhan and B. Balagam, *Macromolecules*, 2006, **39**, 2010-2012.
- ²⁰ H. Nagashima, C. Itonaga, J. Yasuhara, Y. Motoyama and K. Matsubara, *Organometallics*, 2004, **23**, 5779-5786.

-
- 21 P. Atallah, K. B. Wagener and M. D. Schulz, *Macromolecules*, 2013, **46**, 4735–4741.
- 22 A. C. Chruch, J. H. Pawlow and K. B. Wagener, *Macromolecules*, 2002, **35**, 5746-5751.
- 23 A. C. Chruch, J. H. Pawlow and K. B. Wagener, *Macromol. Chem. Phys.*, 2003, **204**, 32-39.
- 24 P. P. Matloka, and K. B. Wagener, *J. Polym. Sci. A: Polym. Chem.*, 2006, **257**, 89-98.
- 25 P. P. Matloka, Z. Kean, M. Greenfield and K. B. Wagener, *J. Polym. Sci. A: Polym. Chem.*, 2008, **46**, 3992-4011.
- 26 P. P. Matloka, J. C. Sworen, F. Zuluaga and K. B. Wagener, *Macromol. Chem. Phys.*, 2005, **206**, 218-226.
- 27 E. Malecka, B. Marciniak, C. Pietraszuk, A. C. Church and K. B. Wagener, *J. Mol. Catal. A: Chem.*, 2002, **190**, 27–31.
- 28 J. C. Marmo and K. B. Wagener, *Macromolecules*, 1995, **28**, 2602–2606.
- 29 K. B. Wagener and J. C. Marmo, *Macromol. Rapid Commun.*, 1995, **16**, 557-561.
- 30 A. K. Diallo, X. Michel, S. Fouquay, G. Michaud, F. Simon, J.-M. Brusson, S. M. Guillaume and J.-F. Carpentier, *Macromolecules*, 2015, **48**, 7453-7465.
- 31 C. W. Bielawski, T. Morita and R. H. Grubbs, *Macromolecules*, 2000, **33**, 678-680.
- 32 M. K. Mahanthappa, F. S. Bates and M. A. Hillmyer, *Macromolecules*, 2005, **38**, 7890-7894.
- 33 B. R. Maughon, T. Morita, C. W. Bielawski and R. H. Grubbs, *Macromolecules*, 2000, **33**, 1929-1935.
- 34 K. Sill and T. Emrick, *J. Polym. Sci. A: Polym. Chem.*, 2005, **43**, 5429-5439.
- 35 H. Martinez and M. A. Hillmyer, *Macromolecules*, 2014, **47**, 479-485.
- 36 C. W. Bielawski, D. Benitez, T. Morita and R. H. Grubbs, *Macromolecules*, 2001, **34**, 8610-8618.
- 37 J. B. Matson and R. H. Grubbs, *Macromolecules*, 2010, **43**, 213-221.
- 38 N. Hanik and A. F. M. Kilbinger, *J. Polym. Sci. A: Polym. Chem.*, 2013, **51**, 4183-4190.
- 39 J. B. Matson, S. C. Virgil and R. H. Grubbs, *J. Am. Chem. Soc.*, 2009, **131**, 3355-3362.
- 40 T. Morita, B. R. Maughon, C. W. Bielawski and R. H. Grubbs, *Macromolecules*, 2000, **33**, 6621-6623.
- 41 L. M. Pitet and Hillmyer, M. A. *Macromolecules*, 2011, **44**, 2378-2381.
- 42 S. Ji, T. R. Hoye and C. W. Macosko, *Macromolecules*, 2004, **37**, 5485-5489.
- 43 S. Ji, T. R. Hoye and C. W. Macosko, *Polymer*, 2008, **49**, 5307-5313.

- 44 L. Annunziata, S. Fouquay, G. Michaud, F. Simon, S. M. Guillaume and J.-F. Carpentier, *Polym. Chem.*, 2013, **4**, 1313-1316.
- 45 L. M. Pitet, M. A. Amendt and M. A. Hillmyer, *J. Am. Chem. Soc.*, 2010, **132**, 8230-8231.
- 46 C. W. Bielawski, O. A. Scherman and R. H. Grubbs, *Polymer*, 2001, **42**, 4939-4945.
- 47 M. A. Hillmyer, S. T. Nguyen and R. H. Grubbs, *Macromolecules*, 1997, **30**, 718-721.
- 48 R. M. Thomas, R. H. Grubbs, *Macromolecules*, 2010, **43**, 3705-3709.
- 49 R. J. P. Corriu, J. J. E. Moreau, P. Thepot and M. W. C. Man, *Chem. Mater.*, 1992, **4**, 1217-1224.
- 50 A. K. Simonian, J. L. Webb, D. J. Brunell, T. E. Banach and S. Rubinsztajn, *Eur. Pat.* 0 900 801, 27.08.1997.
- 51 J. Stein, *US Pat.* 6,296,944, 2001.
- 52 The “non-functionalized” PCOE is made of **CNF** but also of linear polymers which may arise from the direct initiation of ROMP by **G2**, especially when the CTA is not reacting (entries 1 and 11). Linear products may also be formed in small amounts through the eventual decomposition (during workup) of the Ru-activated linear polymer chain such as **II/III** (Scheme 1).
- 53 R. H. Grubbs and M. A. Hillmyer, *Macromolecules*, 1995, **28**, 8662-8667.
- 54 C. Pietraszuk, B. Marciniec, S. Rogalski and H. Fischer, *J. Mol. Catal. A Chem.*, 2005, **240**, 67-71.
- 55 M. Ulman and R. H. Grubbs, *Organometallics*, 1988, **17**, 2484-2489.
- 56 GLC and NMR analyses did not reveal the presence of residual DMAP, which is used in the synthesis of CTAs **3-OMe**, **3-OEt** or **isom-4**. Indeed, DMAP is known to inhibit Ru-based metathesis catalysts: purposely added DMAP (1 equiv vs. [Ru]) lowers 5 times the reactivity of the catalyst, while the ROMP reaction was entirely inhibited using 2 or more equiv of DMAP; see: S. J. P’Poo I and H.-J. Schanz, *J. Am. Chem. Soc.*, 2007, **129**, 14200-14212.
- 57 K. J. Ivin, *J. Mol. Catal. A: Chem.*, 1998, **133**, 1-16.
- 58 K. Yamamoto, K. Biswas, C. Gaula and S. J. Danishefsky, *Tetrahedron Lett.*, 2003, **44**, 3297-3299.
- 59 J. A. Love, J. P. Morgan, T. M. Trnka and R. H. Grubbs, *Angew. Chem., Int. Ed.*, 2002, **41**, 4035-4037.

-
- ⁶⁰ S. B. Garber, J. S. Kingsbury, B. L. Gray and A. H. Hoveyda, *J. Am. Chem. Soc.*, 2000, **122**, 8168-8179.
- ⁶¹ Z.-Y. J. Zhan, *US Pat.* 0043180, 2007
- ⁶² (a) H. Clavier, F. Caijo, E. Borre', D. Rix, F. Boeda, S. P. Nolan and M. Mauduit, *Eur. J. Org. Chem.*, 2009, **25**, 4254-4265. (b) D. Rix, F. Caijo, I. Laurent, F. Boeda, H. Clavier, S. P. Nolan, M. Mauduit, *J. Org. Chem.*, 2008, **73**, 4225-4228.
- ⁶³ A. K. Diallo, L. Annunziata, S. Fouquay, G. Michaud, F. Simon, J.-M. Brusson, S. M. Guillaume and J.-F. Carpentier, *Polym. Chem.*, 2014, **5**, 2583-2591.
- ⁶⁴ C. W. Bielawski, O. A. Scherman and R. H. Grubbs, *Polymer*, 2001, **42**, 4939-4945.
- ⁶⁵ L. M. Pitet and M. A. Hillmyer, *Macromolecules*, 2011, **44**, 2378-2381.

Graphical abstract

